

## ISG & GPS/GNSS 2007

### Estimating of Regional Evapotranspiration for Arid Areas Using LANDSAT Thematic Mapper Images data: A Case Study for Grape Plantation

Ayoub Almhab Ibrahim Busu Nourkhair Ibrahim  
Faculty of Geoinformation science and engineering  
University Teknologi Malaysia  
e-mail: [aalmhap@maktoob.com](mailto:aalmhap@maktoob.com) , [ibusu@fksg.utm.my](mailto:ibusu@fksg.utm.my)

#### 1. Abstract

In west southern mountains of Yemen grape crop has been considered as an important cash crop. Thus, water management for grape plantation in arid areas has become an important aspect to ensure a food produce. Except alfalfa, the water used by grape trees is greater than that of most crops. Conventional Point measurement of water needed by one Grape plantation cannot provide accurate estimate for all the orchards in a county. In fact, over a vast area, the point measurements technique is costly and unpractical. In this paper, a new approach is suggested to estimate detailed water requirement by grape plantation at a county scale. The proposed technique used LANDSAT-TM data and a modified SEBAL (Surface Energy Balance Algorithm for Land) to estimate evapotranspiration over grape plantation in wadi asser- Sana'a basin central Yemen mountains. The modified SEBAL model estimates evapotranspiration (ET) using the energy balance equations, for which the surface temperature and reflectance data from TM image data and metrological data from local weather station. The model calculates net radiation, soil and sensible heat flux, and evapotranspiration. Comparing the calculated results with those observed in point measurements in the field of Grape and alfalfa from the period 1995 to 1998 proves that the modified SEBAL also provides an accurate information. The average relative error between estimated and observed ET is 11.6%, and the average absolute error is 0.43 mm/day. This proposed technique has the potential to provide guidelines for various users, including government agencies on how to evaluate current water-usage schemes.

*Keywords:* Evapotranspiration; Surface energy balance; Yemen

## 2. INTRODUCTION

Since Grape has been an important cash crop for the mountainous areas in western Yemen, its water usage should be carefully managed in order to achieve water and good quality yield from the available water. It exists that water use by Grape trees is greater than that of most row crops, except alfalfa. It's found that Grape has an annual evapotranspiration (ET) of about 1.6m to 2.4m irrigation a year (AREA, 2005). Estimating Grape water usage has been an important research issue, especially in arid areas where water is scarce. In general, the study for water management is based on ground measurements (point measurement) which are laborious and time consuming. Furthermore the reclaiming could not be able to provide an accurate spatial estimation, especially when large area is included. Thus, alternative approach is required to further estimate the study of water usage in Grape plantation. This approach is utilizing satellite images data which are capable of providing large area coverage. Evapotranspiration (ET), as part of the hydrological cycle, is affected by many processes at the interface between soil, vegetation and atmosphere. A number of models for ET estimation have been presented: empirical; semi-empirical models; and physical models. These have increased the precision of ET estimation [Brutsert, 1979].

The empirical methods assume the daily ET and linearly relates to the cumulative temperature difference (surface temperature minus the air temperature) (Caurault, et al., 2003). On a local scale, accuracy could be reached at 85-90% (Steinmetz, et al., 1989). But if the method is used for regional scale, the accuracy will be around 70-80% because the input parameter (air temperature) must be interpolated from local measurement.

SEBAL is one of the residual methods of energy budget, developed by (Bastiaanssen, et al., 1998). It combines empirical and physical parameterization. The inputs include local weather data (mainly wind speed) and satellite data (radiance). From the input data, the  $R_n$  (net solar radiation) and  $G$  (soil heat flux) are calculated. The  $H$  sensible heat flux is calculated by contrasting two points (wet, well-irrigated vegetation and dry ground, desert). Then, the ET is calculated as the residual of the energy budget (Bastiaanssen, et al., 1998). The accuracy can be 85% in daily basis and 95% in seasonal basis (Bastiaanssen, et al., 2005). Based on the contrast of wet and dry areas, similar models like SEBI, -S-SEBI and SEBS were developed (Menenti and Choudhury 1993; Roerrink, et al., 2000; Su 2002).

Semi-empirical models and physical models deal with soil and plant energy exchange with the atmosphere with a fine time step of 1 s to 1 hr (Caurault, et al., 2003). These methods accurately describe crop functioning, and can allow access to the intermediate variables such as soil moisture and LAI (leaf area index), which are related to the physiological and hydraulic processes that can be linked to other meteorological and hydrologic models (Caurault, et al., 2003).

Most of the models use data to obtain the surface temperature and need accurate temperature data. SEBAL avoids the problem (to input accurate surface data) by using the temperature difference between air and ground for each pixel which is scaled by surface temperature in contrast with dry and wet spot values. Thus, SEBAL is more attractive for operational applications (Wing, et al., 2006).

The main objective of this study is to study the feasibility of using SEBAL with different processing levels, LANDSAT5 TM, for 1995 to 1998 season, in order to estimate grape water use by remote sensing over an arid and semi-arid areas with non-homogeneous surface condition in wadi Asser- Sana'a basin- Yemen.

### 3. MATERIALS AND METHODS

#### 3.1. Study area

The Sana'a Basin is located in the western highlands of Yemen opposite the Red Sea and the Gulf of Aden (figure 1). It is mostly an intermountain plain surrounded by highlands from the west, south and east. On a regional scale, the Basin extends across the central part of the Sana'a Governorate (figure 1) and covers about 24% (3250 km<sup>2</sup>) of its total area (13,550km<sup>2</sup>).

There is a significant variation in altitude both east-west and north-south. The highest point in the Basin is in the southwest end (Jabal An Nabi Shu'ayb) and has an elevation of almost 3700 m above sea level (m.a.s.l.) The lowest (about 1900 m.a.s.l.) is in the northern extremity where the Wadi Al Kharid exits the Basin towards the main basin by the same name. The predominant climate is arid although semi-arid conditions prevail in localized areas, particularly along the western highlands, wadi asser is the one from the very important wadi produce the grape in Sana'a basin and in Yemen,.

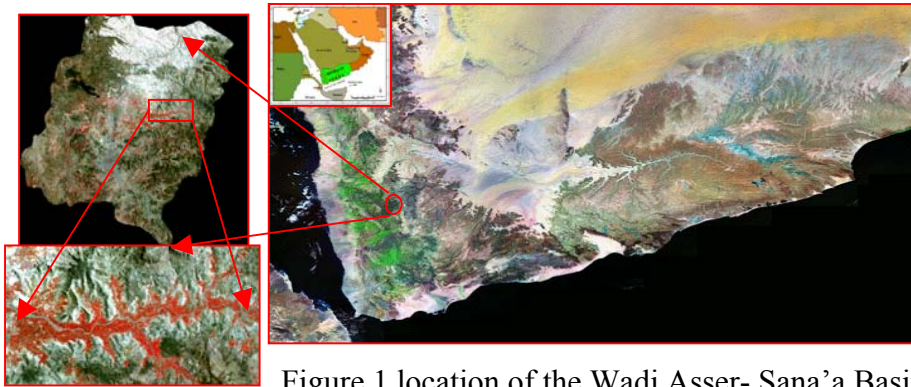


Figure 1 location of the Wadi Asser- Sana'a Basin Yemen mountains

#### 2.2. Dataset

Satellite images LANDSAT5-TM in year95-98, were evaluated for Land Surface Heat Fluxes distribution in Sana'a basin central Yemen mountains. These overpass time of these images was 10.30of LANDSAT5-TM – local time. Both images had favorable weather conditions without or little clouds in the study area. Data from the field measurement area were available to assist the calculation of the Land Surface Heat Fluxes in the locations of the study area (Lat: 15.3 N, long: 43.15 E). Figure 2. show sample from the field measurement, test and gathering the meteorological ground conditions at the study area.



Figure 2 field measurement, test and gathering data from hydro metrological station in different areas in Yemen.

Table 1 National (LANDSAT) acquisition dates during the 95-98ropping season.

Mar 26 1995	Oct 13 1995	June 1 1998
-------------	-------------	-------------

**Model**

**2.3. Model**

A Modified SEBAL model was develop by introducing some changes into the existing SEBAL model .Notably, the inclusion of terrain, mountains and deserts effect in to calculations of surface radiation.

A Modified SEBAL model was calculated using model builder in ERDAS IMAGINE 8.5 image processing package. All model parameters are programmed in to the model builder and values are computed automatically based on the input data. The general flowchart for the modified SEBSL model is shown by Figure 3.

The method uses the energy budget equation to calculate each pixel  $\lambda ET_{ins}$  (instant latent heat loss ) at the time of the satellite over flight.

$$\lambda ET_{ins} = Rn - G - H \quad ((W/m^2)) \quad \text{Eq. 1}$$

Where:

$\lambda ET_{ins}$ : the instant latent heat loss( $w/m^2$ ) , which is calculated as a residual of the energy budget , $\lambda$  is the heat loss when a gram of water evaporates,  $ET_{ins}$  is the rate of evapotranspiter at the time of the satellite overflight,  $Rn$  is net solar raids ( $w/m^2$ ),  $G$  is soil heat flux into the soil ( $w/m^2$ ),  $H$  is sensible heat into the air ( $w/m^2$ ),

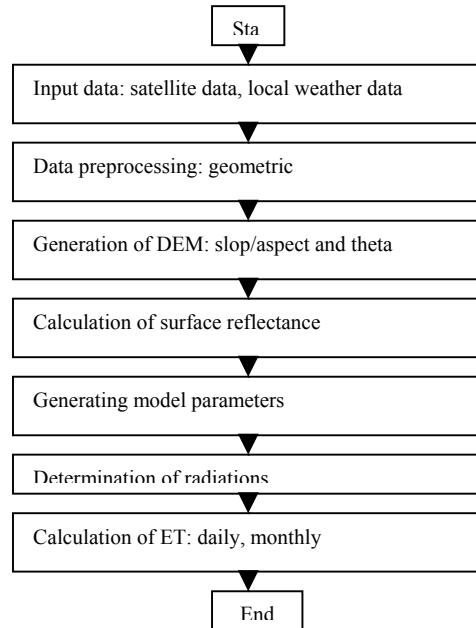


Figure 3 the general flowchart of the modified SEBAL model

**Theory**

**Net Radiation (Rn)**

The radiation balance at the earth’s surface is composed of four spectral radiant fluxes, the incoming short wave (0.14-4  $\mu m$ ) radiation that arrives from the sun ( $Rs\downarrow$ ), the amount of this energy that is reflected from the surface ( $Rs\uparrow$ ), the incoming long wave ( $> 4 \mu m$ ) radiation from the atmosphere ( $RL\downarrow$ ), and the amount of long wave radiation emitted from the surface ( $RL\uparrow$ ). Thus the net radiation is:

$$R_n = R_{s\downarrow} - R_{s\uparrow} + R_{L\downarrow} - R_{L\uparrow} \quad ((\text{W}/\text{m}^2)) \quad \text{Eq. 2}$$

The instantaneous net amount of radiation received by a surface can be written in the form:

$$R_n = (1 - \alpha)R_{s\downarrow} + \varepsilon_a \sigma T_a^4 - \varepsilon_s \sigma T_s^4 \quad ((\text{W}/\text{m}^2)) \quad \text{Eq. 3}$$

where  $R_s$  is the incoming short-wave solar radiation,  $\alpha$ - the surface short-wave albedo,  $\sigma$  the Stefan–Boltzman constant ( $5.67 \times 10^{-8} \text{ w m}^{-2} \text{ K}^{-4}$ ),  $T_a$  is air temperature measured at the wet pixel ( $^{\circ}\text{K}$ ),  $T_s$  derived from a remotely sensed radiometric surface temperature ( $^{\circ}\text{K}$ ),  $\varepsilon_a$  is the air emissivity taking as [Bastiaanssen, 1995]:

$$\varepsilon_a = 1.08 * (-\ln * \tau_{sw})^{0.265} \quad ((\text{W}/\text{m}^2)) \quad \text{Eq. 4}$$

where  $\tau_{sw}(-)$  is two way atmospheric transmissivity [ $\tau_{sw} = 0.75 + 2 \times 10^{-5} z$ ],  $z$  is elevation meter. where  $\varepsilon_s$ = surface emissivity is calculated from normalized vegetation index (NDVI) using the logarithmic relation of Van de Griend and Owe (1993) as:

$$\varepsilon_s = 1.0094 + 0.047 * \ln(\text{NDVI}) \quad ((\text{W}/\text{m}^2)) \quad \text{Eq. 5}$$

The weighting factors for each band are the proportions of solar radiation incident at the earth surface in each segment. His approach was adopted here to derive  $\alpha$  from narrow bands.  $\alpha$  is calculated by the equation in Tasume et al (2000) for LANDSAT surface reflectance data.

$$\begin{aligned} \rho_{\text{TOA}} = & 0.293 \rho_{1\text{TOA}} + 0.274 \rho_{2\text{TOA}} + 0.233 \rho_{3\text{TOA}} \\ & + 0.157 \rho_{4\text{TOA}} + 0.033 \rho_{5\text{TOA}} + 0.011 \rho_{7\text{TOA}} \end{aligned} \quad \text{Eq. 6}$$

$\rho_i$  is the reflectance for LANDSAT data band  $i$ .

The incoming short wave radiation ( $R_{s\downarrow}$ ) was estimated from the equation.

$$R_{s\downarrow} = G_{sc} * \cos \theta * dr * \tau_{sw} \quad ((\text{W}/\text{m}^2)) \quad \text{Eq. 7}$$

Where  $G_{sc}$  is the solar constant ( $1367 \text{ w}/\text{m}^2$ ),  $d_{e-s}$  is inverse squared relative distance earth-sun (dimensionless) calculated by  $dr = 1 + 0.033 \cos(\text{DOY} * 2\pi/365)$ ,  $\cos \theta$  is cosine of the solar zenith angle calculated by  $\cos \theta = \cos(\pi/2 - \Phi)$  where  $\Phi$  is sun elevation angle in radian (in the flat area) in the slop area and mountain solar incident angle changes with surface slop and spect. Therefore the equation sugicton from [Duffie and Bekman, 1991] is applied.

### Soil Heat Flux (G)

Soil heat flux is usually measured with sensors buried just beneath the soil surface. A remote measurement of  $G$  is not possible but several studies have shown that the day time ratio of  $G/R_n$  is related to among other factors, such as the normalized difference vegetation index (NDVI). In this study we have adapted the equation (8) the figure 4 showing the regression equation.

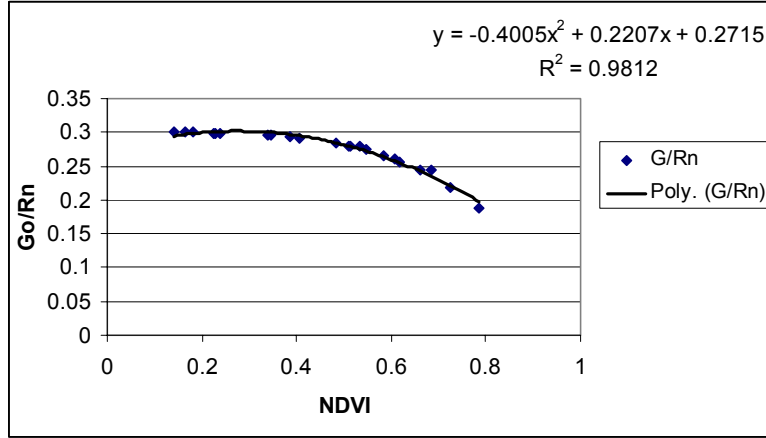


Figure4 the regression equation for  $G/Rn$

$G$  as an empirical fraction of the net radiation using surface temperature, surface albedo ( $\alpha$ ) and NDVI and was adopted here to compute  $G$  as:

$$G = R_n * (-0.4005 \text{ NDVI}^2 + 0.2207 \text{ NDVI} + 0.2715) \quad ((\text{W}/\text{m}^2)) \quad \text{Eq. 8}$$

Where  $T_s$  is the surface temperature, NDVI is the normalized difference vegetation index, is calculated as the following:

$$\text{NDVI} = \frac{r_4 - r_3}{r_4 + r_3} \quad \text{Eq. 9}$$

where  $R_4$  and  $R_3$  are the reflectance data of bands 4 and 3 respectively.

### Sensible Heat Flux

For the sensible heat flux calculation, two pixels are chosen in the satellite data. One pixel is a wet pixel that is a well-irrigated crop surface with full cover and the surface temperature ( $T_s$ ) close to air temperature ( $T_a$ ). The second pixel is a dry bare agricultural field where  $\lambda E$  is assumed to be 0. The two pixels tie the calculations for all other pixels between these two points. At the dry pixel, assume  $\lambda E = 0$ , then according to equation 1,

$$H = Rn - G \quad ((\text{W}/\text{m}^2)) \quad \text{Eq. 10}$$

$$H = \frac{\rho c_p dT}{r_{ah}} \quad ((\text{W}/\text{m}^2)) \quad \text{Eq. 11}$$

Where  $\rho$  is the air density ( $\text{mol}/\text{m}^3$ ),  $C_p$  is the specific heat of air ( $29.3 \text{ J}/\text{mol}/^\circ\text{C}$ ),  $dT$  is the near surface temperature difference (K),  $r_{ah}$  is the aerodynamic resistance to heat transport (s/m), where

$$r_{ah} = \frac{\ln\left(\frac{z_2}{z_1}\right)}{u^* k} \quad \text{Eq. 12}$$

$Z_1$  is a height just above the zero displacement distance height of plant canopy set to 0.1 m for each pixel, and  $Z_2$  is the reference height just above the plant canopy set to 2 m for each pixel,  $u^*$  is the friction velocity (m/s), and  $k$  is the von Karman constant (0.4).

$$u^* = \frac{u(z)k}{\ln\left(\frac{z-d}{z_m}\right)} \quad ((\text{m/s})) \quad \text{Eq.13}$$

Where  $u(z)$  is the wind speed at height of  $z$ ,  $d$  is the zero displacement height (m,  $d=0.65h$ ),  $h$  is the plant height (m), and is the roughness length (m,  $z_m=0.1h$ ) [Campbell and Norman 1998]. According to equations 12-15 and the input data,  $dT_{dry}$ ,  $dT$  at the dry spot can be calculated. At the wet spot, assume  $H=0$  and  $dT_{wet}=0$  ( $dT$  at the wet spot). Then according to the surface temperature at the dry and wet spots ( $T_{s,dry}$  and  $T_{s,wet}$ , K), we can get one linear equation for each pixel (wing et al, 2006),

$$dT = \left( \frac{dT_{dry} - dT_{wet}}{T_{s,dry} - T_{s,wet}} \right) \times T_s - \left( \frac{dT_{dry} - dT_{wet}}{T_{s,dry} - T_{s,wet}} \right) \times T_{s,wet} \quad k \quad \text{Eq. 14}$$

Then, according to the equation, the  $d$  each pixel can be calculated according to equations 13-15. We assumed at 200 m the wind speed is the same for each pixel and the wind speed at 200 m is calculated for the weather station first, and then  $u^*$  can be solved for each pixel (equation 15). The parameter in equation 15 is set to 0 which is negligible when  $z=200$  m. The  $z_m$  for each pixel is calculated by a regression equation according to the pixel value. The equation is obtained by three pair of known values of and. For example if we know that Grape has  $z_m=1.2$  m and  $NDVI=0.57$ , for alfalfa  $z_m=0.07$  m and  $NDVI=0.42$ , and bare agricultural field  $z_m=0.003$  m and  $NDVI=0.18$ , then we can obtain a regression equation for (Figure 2).

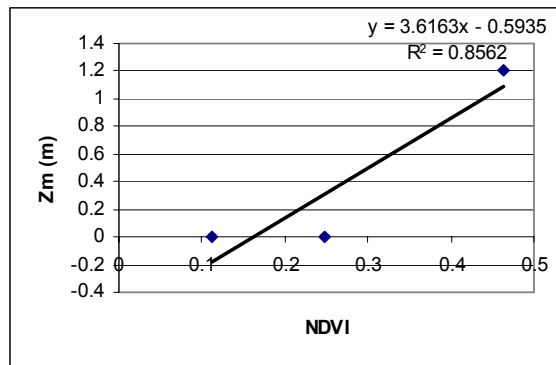


Figure 5. One example regression equation for  $z_m$  from NDVI.

Because atmospheric stability may have effects on  $H$ , the atmospheric correction is conducted. First the  $u^*$  and wind speed at 200 m at the local weather station are calculated. Then the  $z_m$ ,  $u^*$  and  $dT$  for each pixel are computed. Then the  $r_{ah}$  and  $H$  without the atmospheric correction are obtained.

For atmospheric correction, the stability parameter, Obukhov length,  $L$ (m) is calculated. Then using the stability parameter,  $u^*$ ,  $r_{ah}$  and  $H$  are corrected. Then an iteration is conducted for  $L, u^*, r_{ah}$  and  $H$  calculation until  $H$  does not change more than

10%. The correction equations are as the follows (Campbell and Norman 1998; Stull 2001).

$$L = -\frac{u^* T_s}{kgH} \quad \text{Eq. 15}$$

When,  $L < 0$ ,  $H$  is positive and heat is transferred from ground surface to air, under unstable condition; when  $L > 0$ ,  $H$  is negative and heat is transferred from air to ground surface, under stable condition; when  $L = 0$ , no heat flux occurs, and is under neutral condition. Because the satellite overflight occurred at local noon time, the atmosphere should have been unstable. Thus, when (stable) occurred, we forced  $L = 0$  (neutral).

After  $H$  is corrected by the atmospheric effects,  $\lambda ET_{ins}$  for each pixel is calculated using equation 1.

### Regional ET model

The actual 24-h ET can be estimated from the instantaneous evaporative fraction EF, and the daily averaged net radiation,  $R_{24}$  [Tasumi, et al, 2000]:

$$ET_{24} = EF * [R_{n24} * ((2.501 - 0.002361 * T_s) * 106)] \quad \text{mm} \quad \text{Eq. 16}$$

where  $ET_{24}$  is the 24-h actual evaporation (mm/day),  $R_{n24}$  is the 24-h net radiation ( $W/m^2$ ),  $T_s$  the surface temperature ( $C^\circ$ ). The EF is the instantaneous evaporative fraction calculated as:

$$EF = \lambda E / R_n - G_0 \quad ((W/m^2)) \quad \text{Eq. 17}$$

where  $R_n$  is the instantaneous net radiation and  $G_0$  the instantaneous soil heat flux.

Finally, the latent heat flux (LE) may be computed as the residual of the surface energy balance equation (Eq. 1). However, in order to facilitate comparison with the sensible heat flux, use is made of the instantaneous evaporative fraction  $\Lambda$ , defined as follows ( )

$$\Lambda = (R_n - G) / R_n - G \quad \text{Eq. 18}$$

Assuming that the evaporative fraction ( $\Lambda$ ) is constant over the day the daily average sensible heat ( $H_{24}$ ) can be derived from  $\Lambda$  and the daily average net radiation ( $R_{n24}$ ) as follows :

$$H_{24} = (1 - \Lambda) R_{n24} \quad ((W/m^2)) \quad \text{Eq. 19}$$

### Observation and simulation Comparison

The measured and simulated is compared. The relative error is calculated as:

$$RelativeError = \frac{|simulation - observation|}{observation} \quad \text{Eq. 26}$$



The absolute error is calculated as (mm/day):

$$AbsoluteError = |simulation - observation| \quad \text{Eq. 27}$$

The average of the relative error and the absolute error was also calculated, respectively. To see if a day was water-stressed in alfalfa field, the non-stressed (alfalfa, mm/day) calculated by FAO Penman-Monteith equation was compared with the corresponding observation. The was obtained from Yemen NWRA Climate Center. The Grape orchard was always well-irrigated and non stressed.

#### 4. RESULTS AND DISCUSSION

The study has revealed some parameters in modified SEBAL are very sensitive. This can be seen from the values of surface parameters derived from satellite image data.

The following figures show results of data processing for different land surface parameters and calculation of ET for the study area.

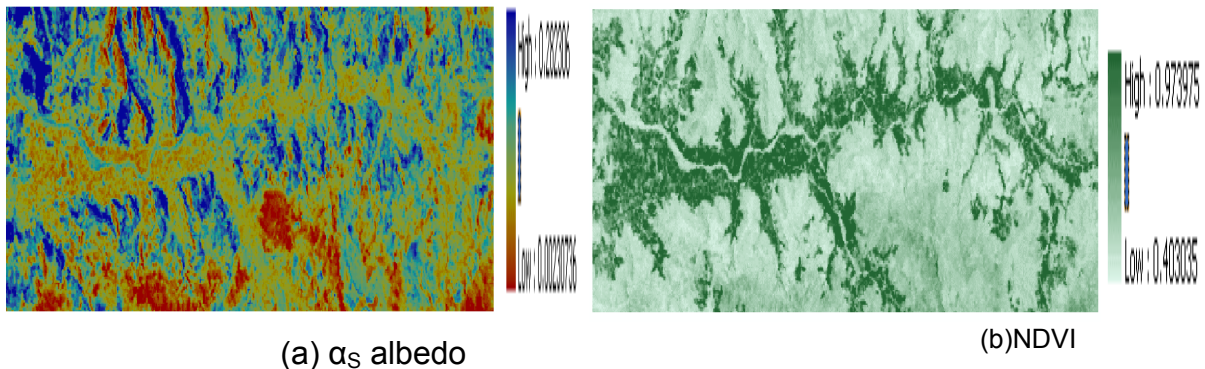
The figures show maximum and minimum values of surface parameters and land surface heat over the study area, which comprises of arid and semi arid conditions.

By comparing figures 6c and 6c it is found that area which high vegetation induces has a low surface temperature. the other land area which have low vegetation indices tends to have high surface temperature. This seen in figure 5b especially the part where there are near the valley which represent the high vegetation density and the part fare from the valley area has the opposite situation.

In this study, figure 6f shows that daily ET is increased from bare soil to where Vegetation indices are high. figure 11 and Table 2 shows comparison between ET derived from LANDSAT5 TM using modified SEBAL and ET calculation using conventional ET models using data from metrological data in Sana'a Basin.

In this study figure 6 (f) shows that daily ET is increased from bare soil to where vegetation indices are high, the daily ET distribution by LANDSAT 5 TM 0.1–9.32 mm.

Figure 9 presents the results of the estimated surface heat fluxes over the study area. The latent heat flux (LE) is increased from bare soil to the vegetated area as ET.



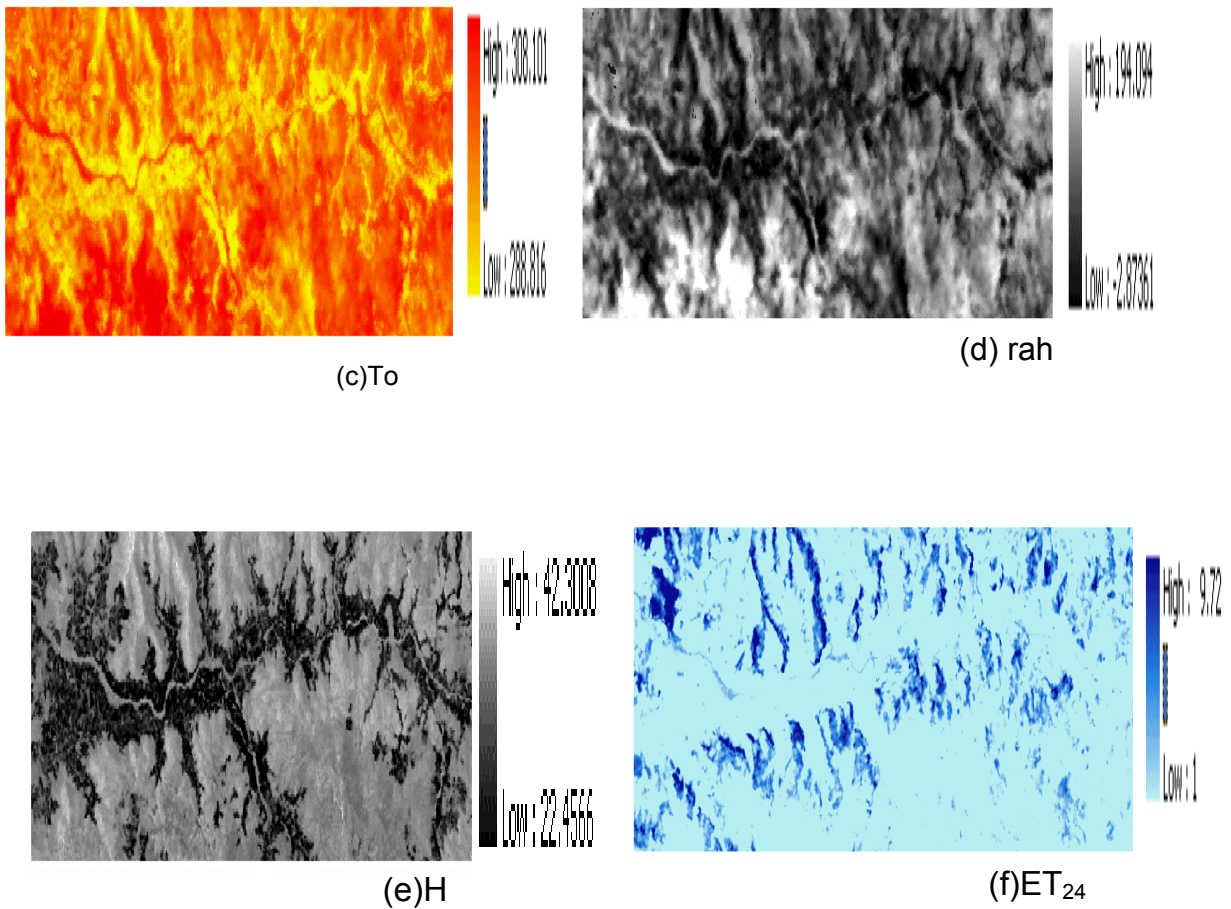


Figure 6 .(a) Estimated surface albedo; (b)vegetation indices (NDVI);(c) Surface Temperature in kelven; (d) airodynamik resistance (e) Sensibole heat flux; (f) evapotranspiration 24 hour driven from LANDSAT 5 TM for wadi asser Sana'a basin Yemen.

Figures 6 and 7 show a positive relationship with vegetation indices ( $y = 14.541(x) + 0.425$ ;  $R^2 = 0.8448$ ), and a negative relationship with land surface temperature ( $y = -0.4031x + 131.07$ ;  $R^2 = 0.8483$ ) in the study area. This relationship is related to the surface moisture conditions in the arid and semi-arid region.

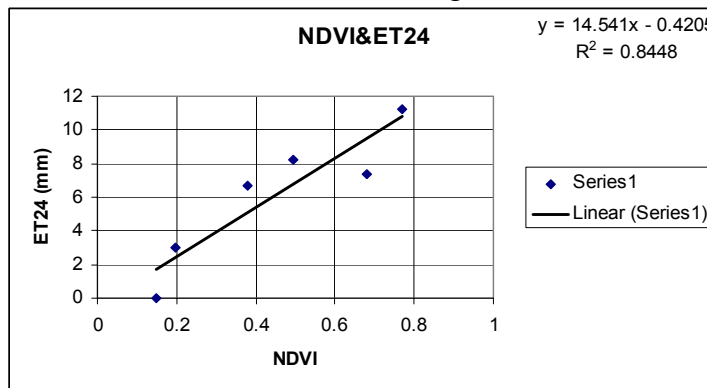


Figure 7. Curve of relationship of daily evapotranspiration (ET24) with vegetation index (NDVI)

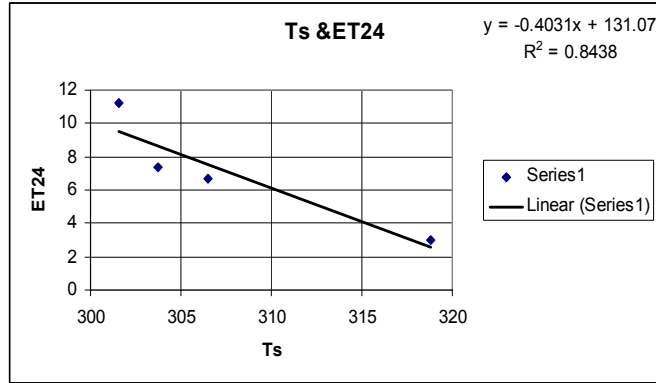


Figure 8. Curve of relationship of daily evapotranspiration (ET24) with land surface temperature (Ts)

Figure 9 show the relationship between the different surface heat fluxes estimated (LE – latent heat flux, Rn-net radiation, G-soil heat flux, H-sensible heat flux) over wadi asser which located in arid and semi-arid region of Sana’a Basin from Landsat 5 TM .

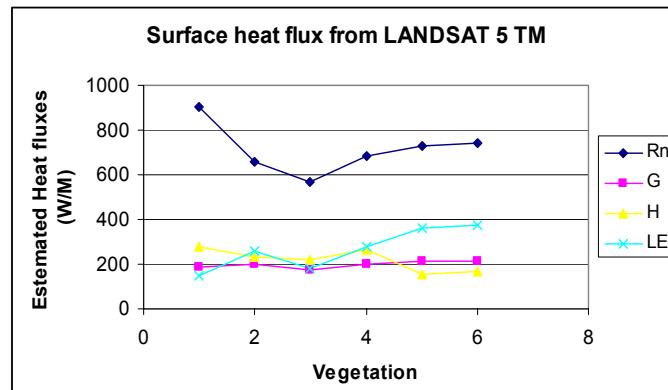


Figure 9. Estimated surface heat fluxes over arid and semi-arid region of Sana’a Basin from Landsat 5 TM . LE –latent heat flux, Rn-net radiation, G-soil heat flux, H-sensible heat flux.

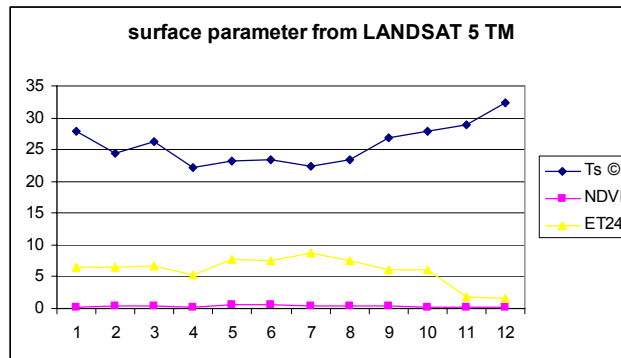


Figure 10. Estimated the surface parameter derived from Landsat 5 on Sana’a Basin from TM, on 1<sup>st</sup> June 1998, Ts surface temperature, NDVI vegetation indices, ET24 evapotranspiration from satellite overpass time.

The model for grape fields is accurate (Table 2, Figure 11). The relative error for GRAPE was 11.9%, 9.8% and 1.6% respectively, for the three satellite over flight days. The absolute errors were within 0.3 mm/day, i.e. 0.5, -0.5, and 0.1 mm/day, respectively.

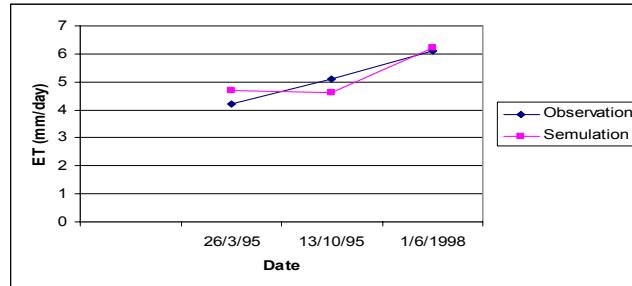


Figure 11. The grape of simulation vs. observation.

Table 2. The alfalfa and grape of simulation vs. observation

Type of Crop	date	observation	simulation	Relative Error	Absolute Error
		ET F.P.M	ET-RS		
Grape	26/03/95	4.2	4.7	0.119	0.5
	13/10/95	5.1	4.6	-0.098	-0.5
	01/06/98	6.1	6.2	0.016	0.1

Ob: observation (mm/day), Si: simulation (mm/day), RE: Relative error, AE: Absolute error (mm/day).

The model can calculate under both stressed and nonstressed conditions accurately. The accuracy is comparable with other studies. For example, using SEBAL model, the daily accuracy can be 85% (Bastiaanssen, et al., 2005).

## 5. CONCLUSION

The modified SEBAL is capable calculating the spatial Grape daily water use (ET) with resolution of 90 m × 90 m. The simulated is accurate compared with measurement under both stressed and no stressed conditions..

This study has been able to demonstrate that some surface parameters such surface albedo, vegetation index, surface temperature and so on can be accurately derived from satellite image data. In this case surface parameters have been derived from LANDSAT 5 TM images captured , with the help of ground truth weather data values of derived surface parameters are validated to gauge the accuracy .

## 6.ACKNOWLEDGMENTS

The authors gratefully acknowledge financial support for this research from the Islamic Development Bank.

## 7. REFERENCES

- Allen, G.R., Pereira, L.S., Raes, D. and Martin, S., 1998, Crop evapotranspiration: guidelines for computing crop water requirements. *FAO Irrigation and Drainage Paper* **56**, 300.
- Bamatraf A.M. 1994, Water Harvesting and conservation system in Yemen , 169-188, in “ Water harvesting for improved agriculture production” FAO Expert consultation Cairo 21-25 november,1993. FAO. Rome. Italy.
- Bastiaanssen, W. G. M., E. J. M. Noordman, H. Pelgrum, G. Davids, B. P. Thoreson, and R. G. Allen, 2005: SEBAL model with remotely sensed data to improve water-resources management under actual field conditions. *J. Irrig Drainage Engin*, 131, 85-93
- Bastiaanssen, W.G.M., 2000, SEBAL-based sensible and latent heat fluxes in the irrigated Gediz Basin, Turkey. *Journal Hydrology* 229(1/2), 87–100.
- Granger, R.J., 1989, Evaporation from natural nonsaturated surfaces. *Journal of Hydrology* 111, 21–29.
- Bastiaanssen, W.G.M., Menenti, M., Feddes, R.A. and Holtslag, A.A.M., 1998, A remote sensing surface energy balance algorithm for land (SEBAL) 1,2. Formulation. *Journal Hydrology* 212/213, 198–212.
- Bastiaanssen, W.G.M., 1995, Regionalization of Surface Flux Densities and Moisture Indicators in Composite Terrain. A Remote Sensing Approach under Clear Skies in Mediterranean Climates (Wageningen: Agricultural Research Department).
- Brutsert, W., 1979, Heat and mass transfer to and from surface with complete vegetation or similar permeable roughness. *Boundary Layer Meteorology* 16, 365–388.
- Burggeman H.X. 1997. Agro climat Resources of Yemen , part 1 , Agro climat inventory , FAO project , gcp,YEM/021/NET,Field doc.11, ministry of agriculture and irrigation , agricultur research and extension authority (AREA), Dhamar, Yemen.
- Caurault, D., B. Seguin, and A. Olios, 2003: Review to estimate evapotranspiration from remote sensing data: some examples from the simplified relationship to the use of mesoscale atmospheric models. ICID workshop on remote sensing of ET for large regions, 17th September, 2003.
- Diaz-Delgado, R., F. Lloret, and X. Pons, 2003: Influence of fire severity on plant regeneration by means of remote sensing imagery. *Int. J. Remote Sensing*, 24, 8, 1751-1763.
- Doorenbos, J. and Pruitt, W.O., 1977, Crop water requirements. *FAO Irrigation and Drainage Paper* 24, 156.
- Kustas, W. P. and J. M. Norman, 2000: A Two-Source Energy Balance Approach Using Directional Radiometric Temperature Observations for Sparse Canopy Covered Surfaces. *Agron J*, 92, 847-854.
- Menenti, M. and B. J. Choudhury, 1993: Parameterization of land surface evapotranspiration using a location dependent potential evapotranspiration and surface temperature range. In *Exchange processes at the land surface for a range of space and time series*, Bolle H.J., R.A. Feddes, and J.D. Kalma (Eds). IAHS Publ, 212, 561-568.
- Miller, D. R., T. W. Sammis, L. J. Simmons, V. P. Gutschick, and J. Wang, 2005: Water use efficiency and net carbon assimilation in a mature irrigated Grape orchard. *Applied Engineering in Agriculture*. In review.
- Roerrink, G. L., B. Su, and D. Martin, 2000: S-SEBI A simple remote sensing algorithm to estimate the surface energy balance. *Phys. Chim Earth (B)*, 25, 147-157.

Sammis, T. W., J. G. Mexal, and D. R. Miller, 2004: Evapotranspiration of flood-irrigated Grapes. *Agricultural Water Manage*, 56, 179-190.

Steinmetz, S., J. P. Lagouarde, R. Delecolle, M. Guerif, and B. Seguin, 1989: Evaporation and water stress using thermal infrared measurements. A general review and a case study on winter durum wheat in southern France. Symposium on physiology breeding of winter cereals for stressed mediterranean environments, ICARDA-INRA.

Stull, R. B., 2001: An introduction to boundary layer meteorology. Kluwer Academic.

Su, Z., 2002: The surface energy balance system (SEBS) for estimation of turbulent heat fluxes. *Hydrology Earth Syste Scie*, 6, 85-99.

Tasumi, M., Bastiaanssen, W.G.M. and Allen, R.G., 2000, Application of the EBAL methodology for estimating consumptive use of water and stream flow depletion in the Bear River Basin of Idaho through remote sensing. EOSDIS Project Final Report, Appendix C.

Van de Griend, A.A. and Owe, M., 1993, On the relationship between thermal emissivity and the normalized divergence vegetation index for natural surfaces. *International Journal of Remote Sensing* 14, 1119–1131.

Vidal A. and Perrier, A, 1989, Analysis of simplified relation used to estimate daily evapotranspiration from satellite thermal IR data. *International Journal of Remote Sensing* 10(8), 1327–1337.

Wing J, Sammis T.W, Meier C.A, Simmons L.J, Miller D.R, Samani Z, 2006, A Modified SEBAL model for spatially estimating pecan consumptive water use for las cruces, New Mexico, Agronomy and Horticulture Departement, New Mexico State Univ.,las Cruses, New Mexico, USA.

Walter, I. A., R. G. Allen, R. Elliott, Itenfisu, D. P. Brown, M. E. Jensen, B. Mecham, T. A. Howell, R. Snyder, S. Eching, T. Spofford, M. Hattendorf, D. Martin, R. H. Cuenca, and J. L. Wright, 2002: ASCE Standardized Reference Evapotranspiration Equation. Environmental and Water Resources Institute of the American Society of Civil Engineers Standardization of Reference Evapotranspiration Task Committee.